

Note after first publication: This document replaces the version originally published on 23/08/2023, which had errors in Fig. **S16** and **S20**.

Supporting information for

**Single molecule magnet feature in luminescent lanthanide
coordination polymers with heptacoordinate Dy/Yb(III) ions as nodes**

Xiang-Tao Dong,^a Meng-Qing Yu,^a Yong-Bo Peng,^a Guo-Xing Zhou,^a Guo Peng,^{a*}
and Xiao-Ming Ren^{a*}

^a State Key Laboratory of Materials-Oriented Chemical Engineering, School of
Chemistry and Molecular Engineering, Nanjing Tech University, Nanjing 211816, P.
R. China

E-mail: guopeng@njtech.edu.cn, xmren@njtech.edu.cn

Table S1. Crystallographic data and structure refinement for complexes **1** and **3**.

	1-Dy	3-Dy ₂
Formula	C ₃₃ H ₂₈ DyN ₃ O ₁₁	C ₃₁ H ₂₃ N ₂ DyO ₉
<i>M_r</i> (g mol ⁻¹)	805.10	730.0224
Crystal system	triclinic	triclinic
Space group	P-1	P-1
<i>T</i> (K)	172.9	196
<i>a</i> (Å)	10.2143(2)	8.2589(9)
<i>b</i> (Å)	11.5890(3)	12.0063(12)
<i>c</i> (Å)	14.0639(4)	13.9780(15)
<i>α</i> (°)	67.399(1)	94.689(2)
<i>β</i> (°)	82.544(1)	101.600(2)
<i>γ</i> (°)	78.428(1)	95.591(2)
<i>V</i> (Å ³)	1503.15(7)	1344.0(3)
<i>Z</i>	2	2
<i>D_c</i> (g cm ⁻³)	1.7787	1.8039
<i>μ</i> (mm ⁻¹)	2.556	2.843
<i>F</i> (000)	802.2	722.2
Reflns collected	16260	9207
Unique reflns	5510	6037
<i>R</i> _{int}	0.0275	0.0320

GOF	1.121	1.036
$R_1(I > 2\sigma)$	0.0252	0.0365
w R_2 (all data)	0.0598	0.0813
Max. diff. peak / hole ($e \text{ \AA}^{-3}$)	2.17/-0.86	1.81/-1.37

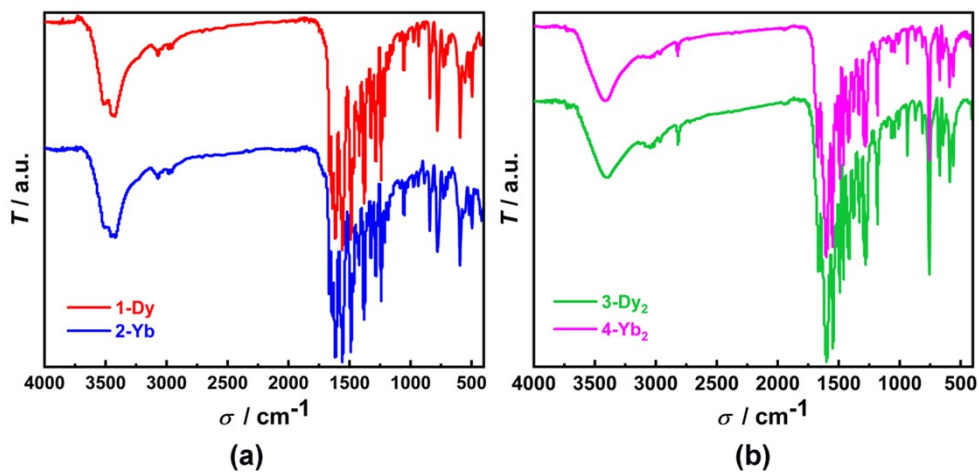


Fig. S1 IR spectra of complexes 1-4.

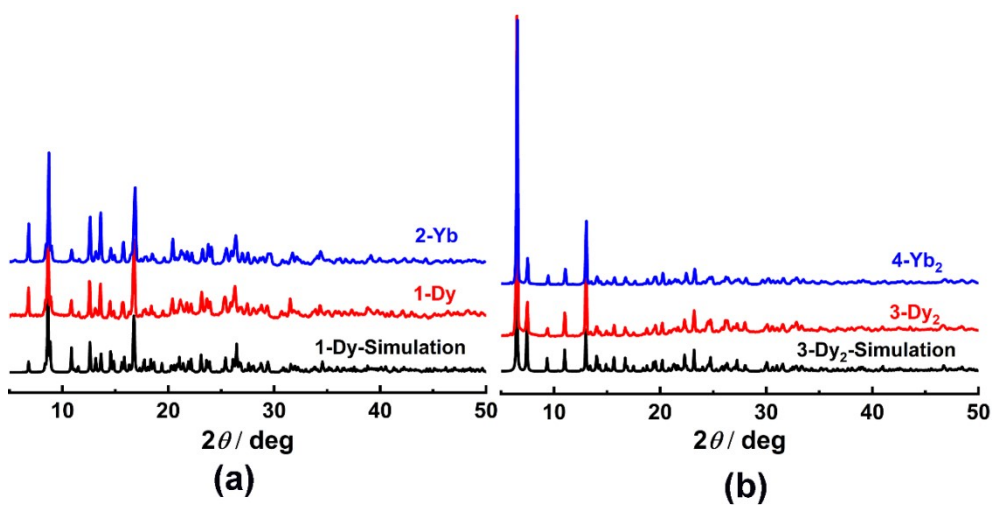


Fig. S2 Measured and simulated PXRD patterns of complexes 1-4.

Table S2. Selected bond lengths (Å) and angles (°) for **1** and **3**.

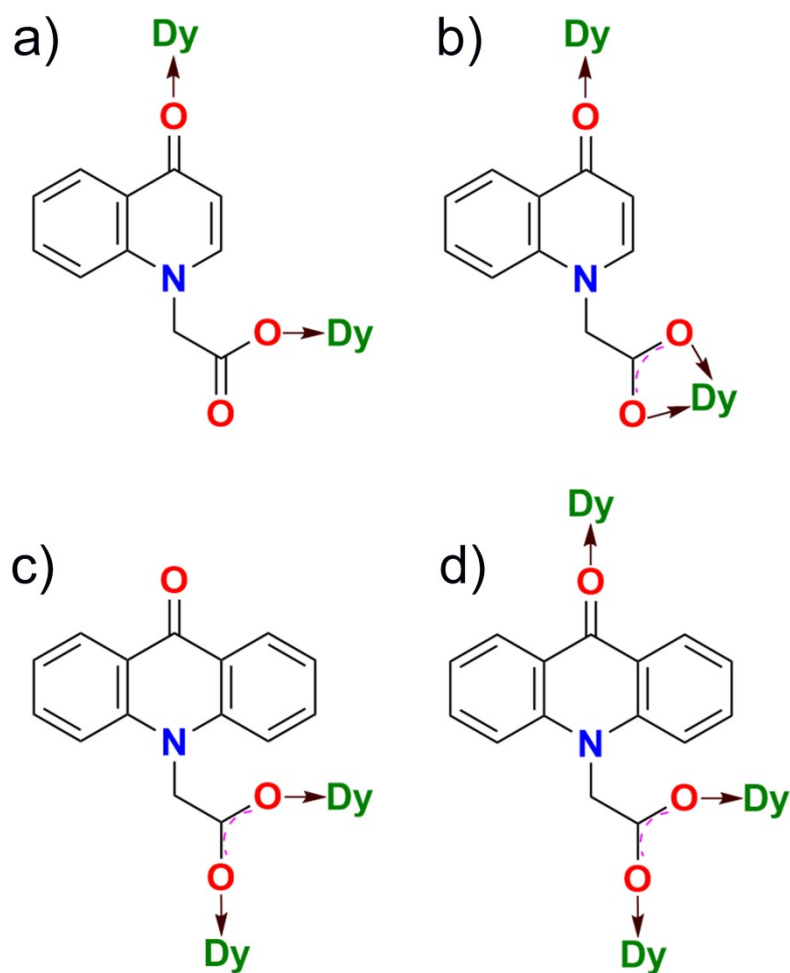
	1		3
Dy(1)-O(1)			
Dy(1)-O(3)#1			
Dy(1)-O(4)			
Dy(1)-O(6)#2	2.197(2)	Dy(1)-O(1)#1	2.356(3)
Dy(1)-O(7)	2.241(2)	Dy(1)-O(2)#3	2.327(3)
Dy(1)-O(8)#2	2.284(2)	Dy(1)-O(3)	2.258(3)
Dy(1)-O(9)#2	2.291(2)	Dy(1)-O(4)	2.278(3)
O(1)-Dy(1)-O(3)#1	2.293(2)	Dy(1)-O(5)#4	2.338(3)
O(1)-Dy(1)-O(4)	2.535(2)	Dy(1)-O(7)	2.374(3)
O(1)-Dy(1)-O(6)#2	2.466(3)	Dy(1)-O(8)	2.254(3)
O(1)-Dy(1)-O(7)	178.63(10)	O(1)#1-Dy(1)-O(7)	79.40(11)
O(1)-Dy(1)-O(8)#2	92.68(10)	O(2)#3-Dy(1)-O(1)#1	128.44(10)
O(1)-Dy(1)-O(9)#2	94.50(10)	O(2)#3-Dy(1)-O(5)#4	74.70(12)
O(3)#1-Dy(1)-O(4)	92.55(10)	O(2)#3-Dy(1)-O(7)	135.24(12)
O(3)#1-Dy(1)-O(6)#2	86.89(9)	O(3)-Dy(1)-O(1)#1	155.95(11)
O(3)#1-Dy(1)-O(7)	97.04(9)	O(3)-Dy(1)-O(2)#3	75.56(11)
O(3)#1-Dy(1)-O(8)#2	87.38(10)	O(3)-Dy(1)-O(4)	104.02(13)
O(3)#1-Dy(1)-O(9)#2	86.84(9)	O(3)-Dy(1)-O(5)#4	110.60(13)
O(4)-Dy(1)-O(6)#2	86.11(9)	O(3)-Dy(1)-O(7)	80.86(11)
O(4)-Dy(1)-O(7)	93.70(9)	O(4)-Dy(1)-O(1)#1	83.42(12)
O(4)-Dy(1)-O(8)#2	82.38(10)	O(4)-Dy(1)-O(2)#3	75.93(12)
O(4)-Dy(1)-O(9)#2	77.38(8)	O(4)-Dy(1)-O(5)#4	126.39(13)
O(6)#2-Dy(1)-O(7)	81.29(9)	O(4)-Dy(1)-O(7)	73.64(12)
O(6)#2-Dy(1)-O(8)#2	151.83(8)	O(5)#4-Dy(1)-O(1)#1	81.15(12)
O(6)#2-Dy(1)-O(9)#2	155.21(9)	O(5)#4-Dy(1)-O(7)	149.96(12)
O(6)#2-Dy(1)-O(8)#2	157.80(9)	O(8)-Dy(1)-O(1)#1	82.80(12)
O(6)#2-Dy(1)-O(9)#2	74.58(8)	O(8)-Dy(1)-O(2)#3	131.50(12)
O(8)#2	124.21(8)	O(8)-Dy(1)-O(3)	80.18(13)
O(6)#2-Dy(1)-O(8)#2	126.89(8)	O(8)-Dy(1)-O(4)	151.53(13)
O(6)#2-Dy(1)-O(9)#2	75.56(8)	O(8)-Dy(1)-O(5)#4	75.62(12)
O(7)-Dy(1)-O(8)#2	51.96(8)	O(8)-Dy(1)-O(7)	79.40(12)
O(7)-Dy(1)-O(9)#2			
O(9)#2-Dy(1)-O(8)#2			

Symmetry codes: #1 x, y+1, z; #2 x+1, y, z; #3 -x+1, -y+1, -z+1; #4 -x+1, -y+2, -z+1.

Table S3. Continuous shape measures (CShM) for complexes 1-Dy and 3-Dy₂.

	1-Dy	3-Dy ₂
HP-7	32.151	32.721
HPY-7	22.424	20.881
PBPY-7	1.417	5.662
COC-7	5.491	0.577
CTPR-7	3.912	1.061
JPBPY-7	4.085	9.111
JETPY-7	22.075	19.120

HP-7=Heptagon, HPY-7=Hexagonal pyramid, **PBPY-7=Pentagonal bipyramid**, **COC-7=Capped octahedron**, CTPR-7=Capped trigonal prism, JPBPY-7=Johnson pentagonal bipyramid J13, JETPY-7=Johnson elongated triangular pyramid J7



Scheme S1. The coordination modes of Hoqa (a, b) and Hoaa (c, d).

Table S4. Intermolecular O/C-H \cdots O hydrogen bonds in **1** and **3** [\AA and $^\circ$].

Complex	D-H \cdots A	d(D-H)	d(H \cdots A)	d(D \cdots A)	\angle (DHA)
1	O(10)-H(10A) \cdots O(5)	0.87	1.98	2.831(4)	166
	O(10)-H(10B) \cdots O(8)	0.87	2.04	2.860(4)	157
	O(11)-H(11A) \cdots O(10)	0.87	2.01	2.834(4)	157
	O(11)-H(11B) \cdots O(2)	0.87	2.01	2.839(5)	159
	C(2)-H(2A) \cdots O(9)	0.99	2.46	3.185(5)	129
	C(2)-H(2B) \cdots O(5)	0.99	2.45	3.311(5)	145
	C(3)-H(3) \cdots O(7)	0.95	2.50	3.453(5)	178
	C(3)-H(3) \cdots O(9)	0.95	2.58	3.016(5)	109
	C(15)-H(15) \cdots O(3)	0.95	2.54	3.314(4)	139
	C(19)-H(19) \cdots O(11)	0.95	2.49	3.294(6)	142
	C(20)-H(20) \cdots O(2)	0.95	2.46	3.356(6)	158
	C(24)-H(24B) \cdots O(10)	0.99	2.43	3.421(5)	176
3	O(7)-H(7A) \cdots O(8)	0.87	2.58	3.100(5)	120
	O(7)-H(7A) \cdots O(9)	0.87	1.95	2.799(5)	164
	O(7)-H(7B) \cdots O(1)	0.87	2.00	2.823(5)	158
	C(2)-H(2A) \cdots O(8)	0.99	2.59	3.471(6)	149
	C(5)-H(5) \cdots O(6)	0.95	2.58	3.523(8)	174
	C(17)-H(17B) \cdots O(9)	0.82(5)	2.55(5)	3.228(7)	142(6)

Table S5. Parameters of π - π interactions in complexes **1** and **3**.

complex	interactions	Dcc (\AA)	Dpp (\AA)	α ($^\circ$)	β ($^\circ$)
1	Cg(3) \cdots Cg(3)	3.420(2)	3.2481(14)	0.00(17)	18.2
	Cg(7) \cdots Cg(7)	4.019(2)	3.5034(16)	0.00(19)	29.3
3	Cg(1) \cdots Cg(1)	4.080(3)	3.596(2)	0.0(2)	28.2
	Cg(1) \cdots Cg(3)	3.926(3)	3.639(2)	3.8(2)	25.4
	Cg(1) \cdots Cg(4)	3.887(3)	3.6514(19)	2.8(2)	18.8
	Cg(2) \cdots Cg(6)	3.547(3)	3.525(2)	1.7(3)	6.8
	Cg(3) \cdots Cg(4)	4.053(3)	3.553(2)	6.1(3)	32.5

For **1**: Cg(3)= six-membered ring N(2)-C(14)-C(15)-C(16)-C(17)-C(22), Cg(7)= six-membered ring C(28)-C(29)-C(30)-C(31)-C(32)-C(33); for **3**: Cg(1)= six-membered ring N(1)-C(3)-C(8)-C(9)-C(10)-C(15), Cg(2)= six-membered ring N(2)-C(18)-C(23)-C(24)-C(25)-C(30), Cg(3)= six-membered ring C(3)-C(4)-C(5)-C(6)-C(7)-C(8), Cg(4)= six-membered ring C(10)-C(11)-C(12)-C(13)-C(14)-C(15), Cg(6)= six-membered ring C(25)-C(26)-C(27)-C(28)-C(29)-C(30). Dcc: the distances between two centers of six-membered rings, Dpp: perpendicular distance between the ring planes, α : dihedral angle between the two planes, β : the angle between the ring normal vectors and the centroid-centroid vectors (Dcc).

Table S6. Static magnetic data for **1-4**.

Compounds	Ground state of Ln(III)	Expected χT at 300 K (cm ³ Kmol ⁻¹)	Measured χT at 300 K (cm ³ Kmol ⁻¹)	Saturation magnetization (N β)	Measured magnetization at 2 K and 7 T (N β)
1-Dy	⁶ H _{15/2}	14.17	14.59	10	5.52
2-Yb	² F _{7/2}	2.57	1.97	4	1.65
3-Dy ₂	⁶ H _{15/2}	28.34	30.63	20	11.42
4-Yb ₂	² F _{7/2}	5.14	4.76	8	3.78

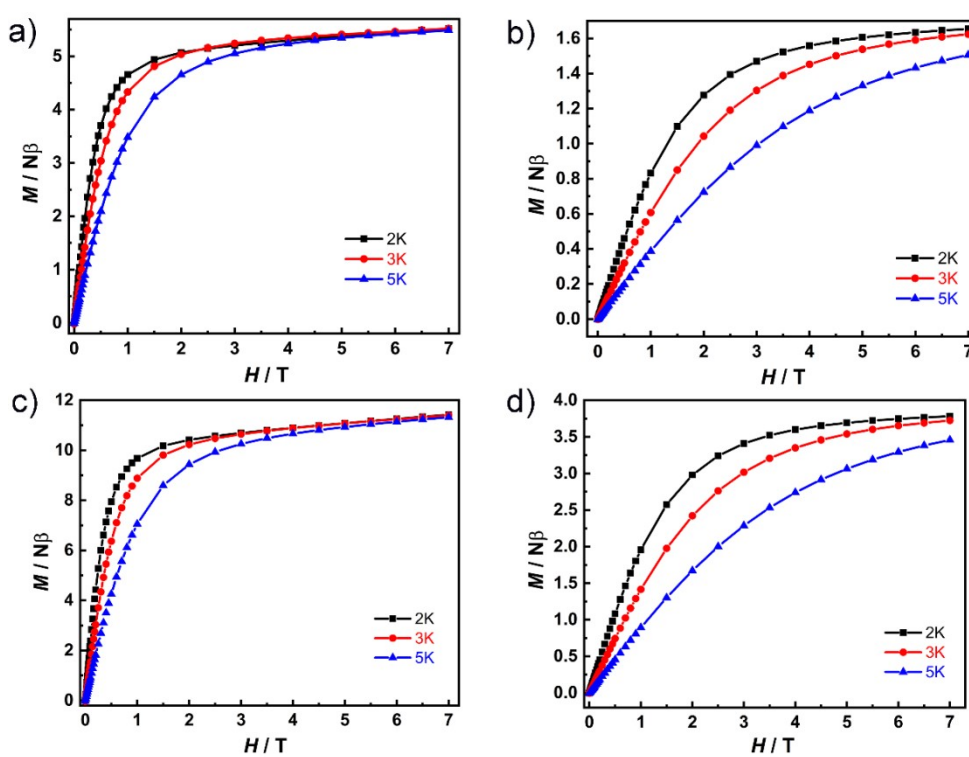


Fig. S3 M vs. H plots for **1-4** (a-d).

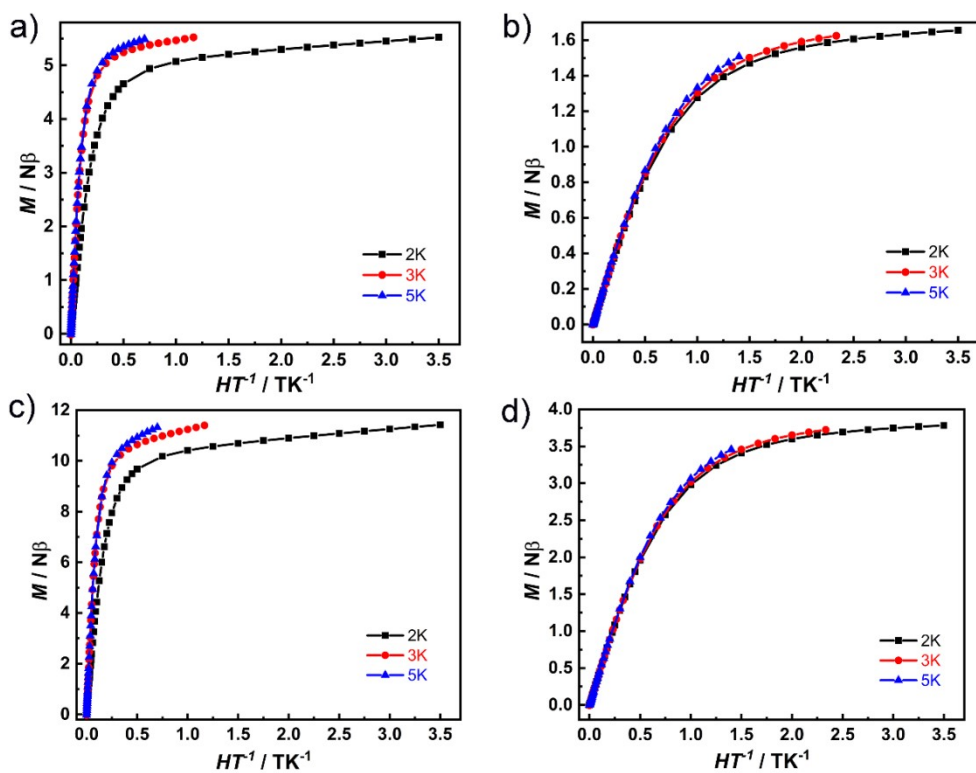


Fig. S4 M vs. HT^{-1} plots for 1-4 (a-d).

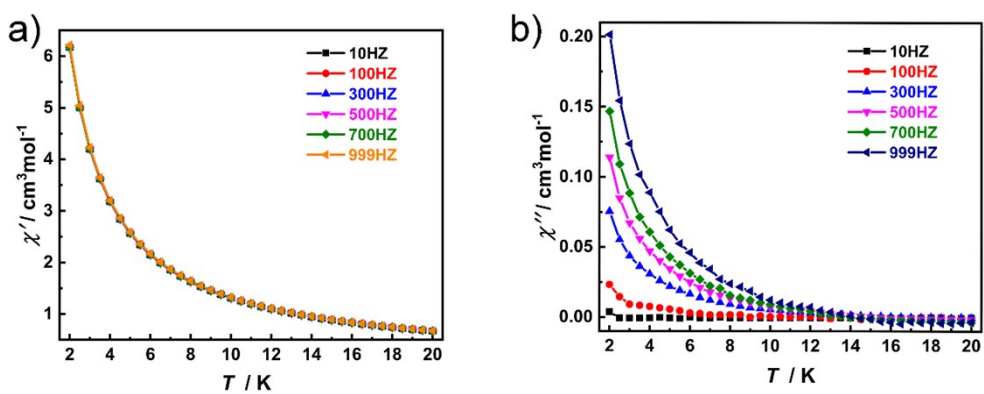


Fig. S5 Temperature dependence of in-phase (a) and out-of-phase (b) ac susceptibility data at a zero dc field for 1.

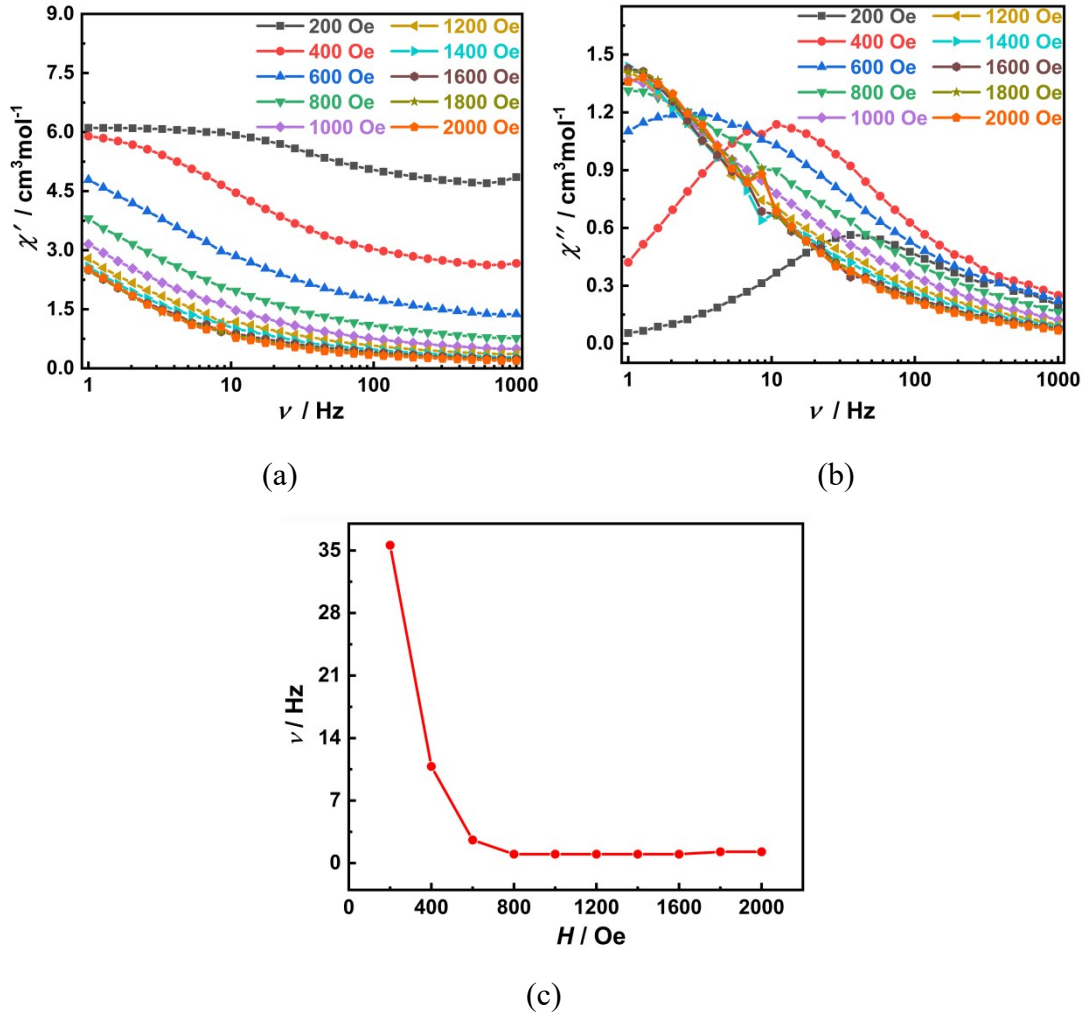


Fig. S6 Frequency dependence of in-phase (a) and out-of-phase (b) ac susceptibility signals under different dc fields at 2K for **1**. Field dependence of the characteristic frequency for **1** at 2K (c).

Table S7. Cole-Cole parameters of **1** under 1000 Oe dc field.

T / K	$\chi_S / \text{cm}^3 \text{mol}^{-1}$	$\chi_T / \text{cm}^3 \text{mol}^{-1}$	τ / s	α	R
2.4	2.63E-01	7.02E+00	4.86E-01	5.96E-01	2.21E-02
2.8	2.55E-01	5.75E+00	2.70E-01	5.92E-01	3.54E-02
3.2	3.02E-01	5.08E+00	1.76E-01	5.52E-01	4.78E-02
3.6	3.47E-01	4.01E+00	6.76E-02	4.72E-01	4.78E-02
4	4.01E-01	3.22E+00	2.71E-02	3.41E-01	9.63E-02
4.4	4.05E-01	2.68E+00	1.31E-02	2.39E-01	8.24E-02
4.8	3.80E-01	2.44E+00	7.82E-03	1.93E-01	5.20E-02
5.2	3.59E-01	2.24E+00	4.84E-03	1.53E-01	3.48E-02
5.6	3.39E-01	2.08E+00	3.11E-03	1.25E-01	2.93E-02
6	3.21E-01	1.94E+00	2.10E-03	1.06E-01	1.40E-02
6.4	3.09E-01	1.81E+00	1.44E-03	8.45E-02	1.43E-02
6.8	2.99E-01	1.71E+00	1.03E-03	6.92E-02	6.60E-03

7.2	2.88E-01	1.62E+00	7.53E-04	6.00E-02	8.41E-03
7.6	2.84E-01	1.53E+00	5.66E-04	5.01E-02	7.82E-03
8	2.71E-01	1.47E+00	4.33E-04	5.24E-02	3.29E-03
8.4	2.63E-01	1.40E+00	3.34E-04	4.71E-02	4.32E-03
8.8	2.53E-01	1.34E+00	2.62E-04	4.99E-02	3.96E-03
9.2	2.54E-01	1.28E+00	2.09E-04	4.10E-02	2.73E-03
9.6	2.66E-01	1.22E+00	1.71E-04	2.35E-02	4.95E-03
10	2.64E-01	1.18E+00	1.38E-04	2.65E-02	3.76E-03

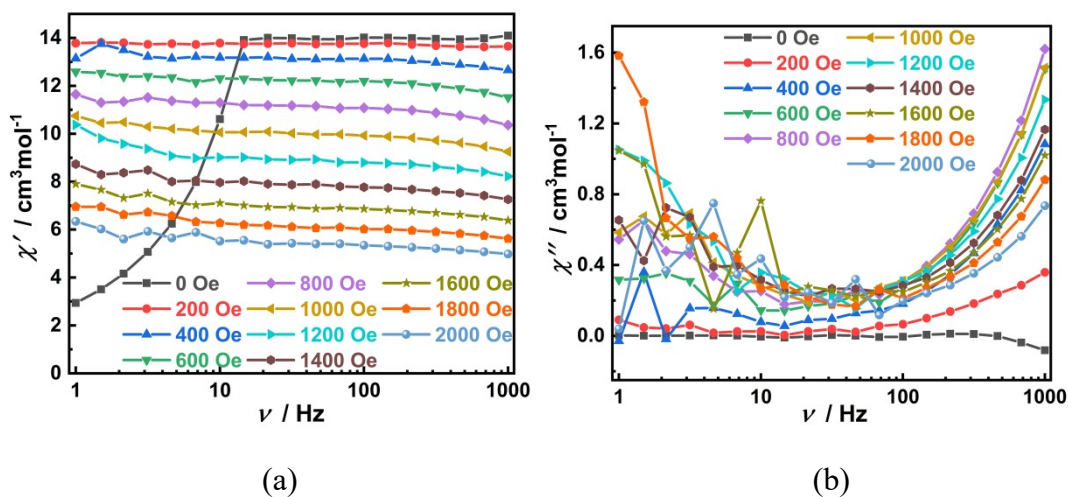


Fig. S7 Frequency dependence of in-phase (a) and out-of-phase (b) ac susceptibility signals under different dc fields at 2K for **3**.

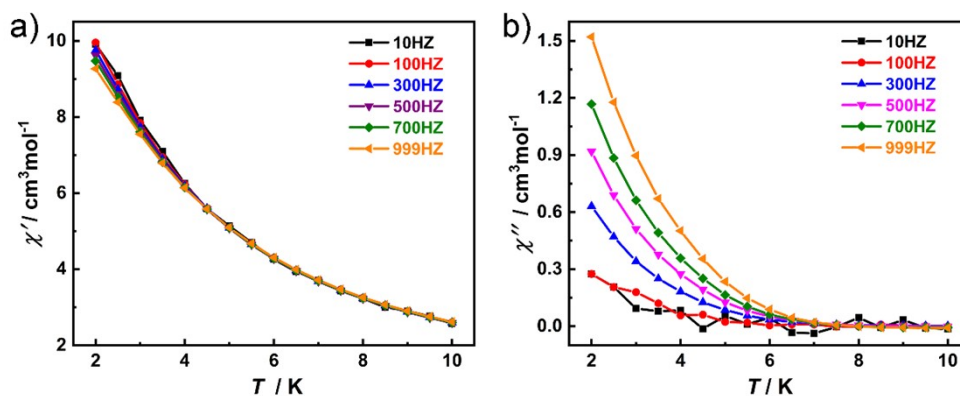


Fig. S8 Temperature dependence of in-phase (a) and out-of-phase (b) ac susceptibility data at a 800 Oe dc field for **3**.

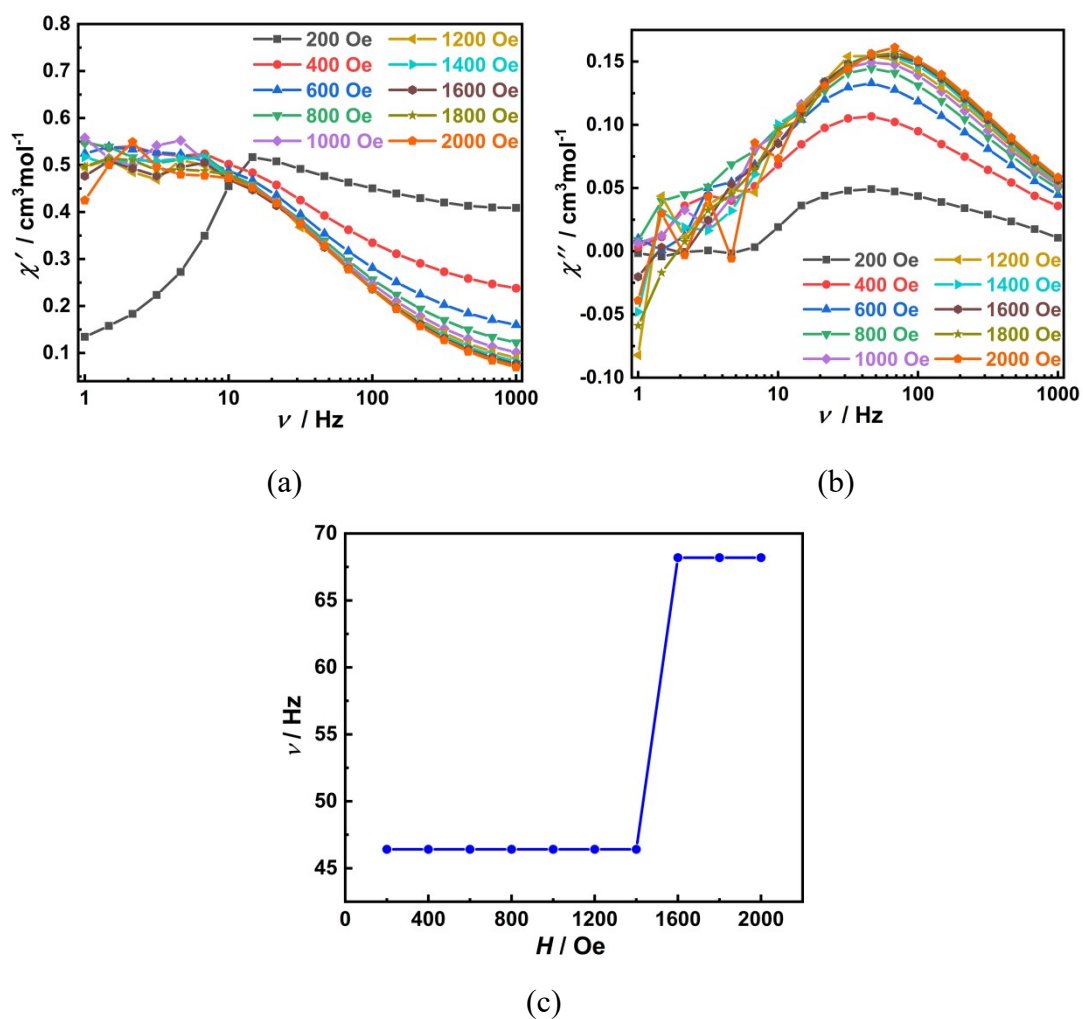
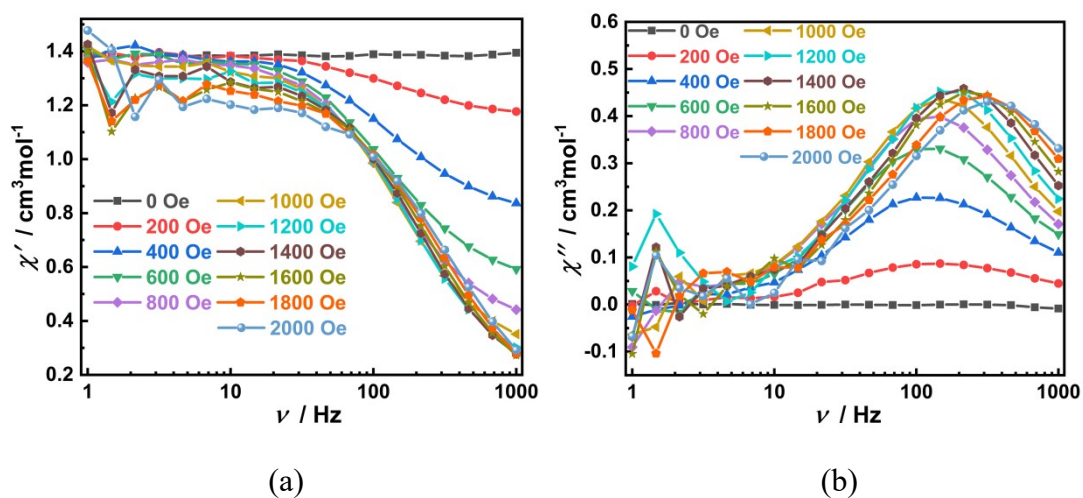
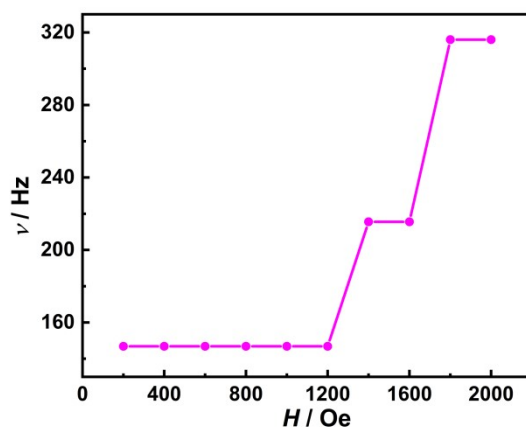


Fig. S9 Frequency dependence of in-phase (a) and out-of-phase (b) ac susceptibility signals under different dc fields at 2K for **2**. Field dependence of the characteristic frequency for **2** at 2K (c).





(c)

Fig. S10 Frequency dependence of in-phase (a) and out-of-phase (b) ac susceptibility signals under different dc fields at 2K for **4**. Field dependence of the characteristic frequency for **4** at 2K (c).

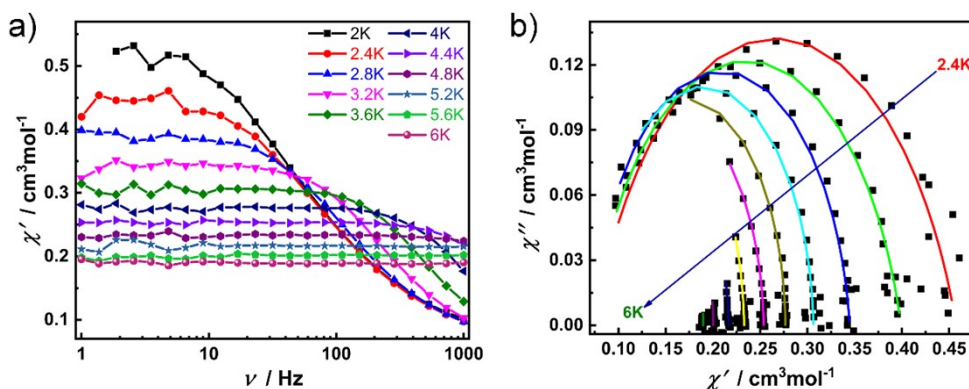


Fig. S11 Frequency dependence of in-phase (a) ac susceptibility data under a 1200 Oe dc field for **2**. Cole–Cole plots for **2** (b). The solid lines are the best fits to a generalized Debye model.

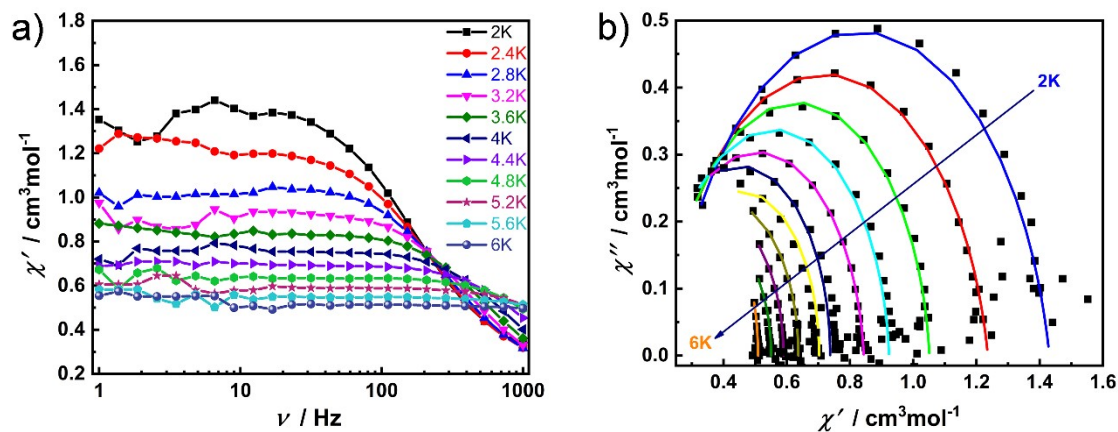


Fig. S12 Frequency dependence of in-phase (a) ac susceptibility data under a 1200 Oe dc field for **4**. Cole–Cole plots for **4** (b). The solid lines are the best fits to a generalized Debye model.

Table S8. Cole-Cole parameters of **2** under 1200 Oe dc field.

T / K	$\chi_S / \text{cm}^3 \text{mol}^{-1}$	$\chi_T / \text{cm}^3 \text{mol}^{-1}$	τ / s	α	R
2.4	7.45E-02	4.57E-01	1.89E-03	2.31E-01	4.17E-03
2.8	7.20E-02	3.99E-01	1.20E-03	1.84E-01	8.69E-04
3.2	7.32E-02	3.45E-01	6.40E-04	9.42E-02	1.34E-03
3.6	7.42E-02	3.06E-01	3.19E-04	3.37E-02	1.09E-03
4	6.43E-02	2.77E-01	1.50E-04	1.16E-02	6.61E-04
4.4	4.68E-02	2.54E-01	6.88E-05	2.37E-02	3.22E-04
4.8	8.76E-06	2.33E-01	2.78E-05	2.68E-02	2.62E-04
5.2	1.85E-05	2.17E-01	1.40E-05	3.02E-02	4.80E-04
5.6	5.60E-06	2.00E-01	8.45E-06	4.80E-15	3.44E-04
6	1.03E-05	1.90E-01	4.43E-06	5.37E-15	1.89E-04

Table S9. Cole-Cole parameters of **4** under 1200 Oe dc field.

T / K	$\chi_S / \text{cm}^3 \text{mol}^{-1}$	$\chi_T / \text{cm}^3 \text{mol}^{-1}$	τ / s	α	R
2	2.30E-01	1.43E+00	9.22E-04	1.37E-01	9.09E-02
2.4	2.05E-01	1.24E+00	7.01E-04	1.29E-01	4.42E-02
2.8	2.15E-01	1.05E+00	5.26E-04	6.44E-02	5.96E-02
3.2	1.96E-01	9.24E-01	3.83E-04	4.84E-02	2.46E-02
3.6	1.72E-01	8.44E-01	2.79E-04	6.36E-02	3.29E-02
4	1.71E-01	7.37E-01	2.00E-04	1.84E-14	6.56E-02
4.8	1.79E-01	6.37E-01	1.09E-04	5.19E-14	1.55E-02
5.2	1.64E-01	5.89E-01	7.53E-05	1.09E-13	1.99E-02
5.6	1.85E-01	5.51E-01	5.60E-05	1.72E-13	2.00E-02

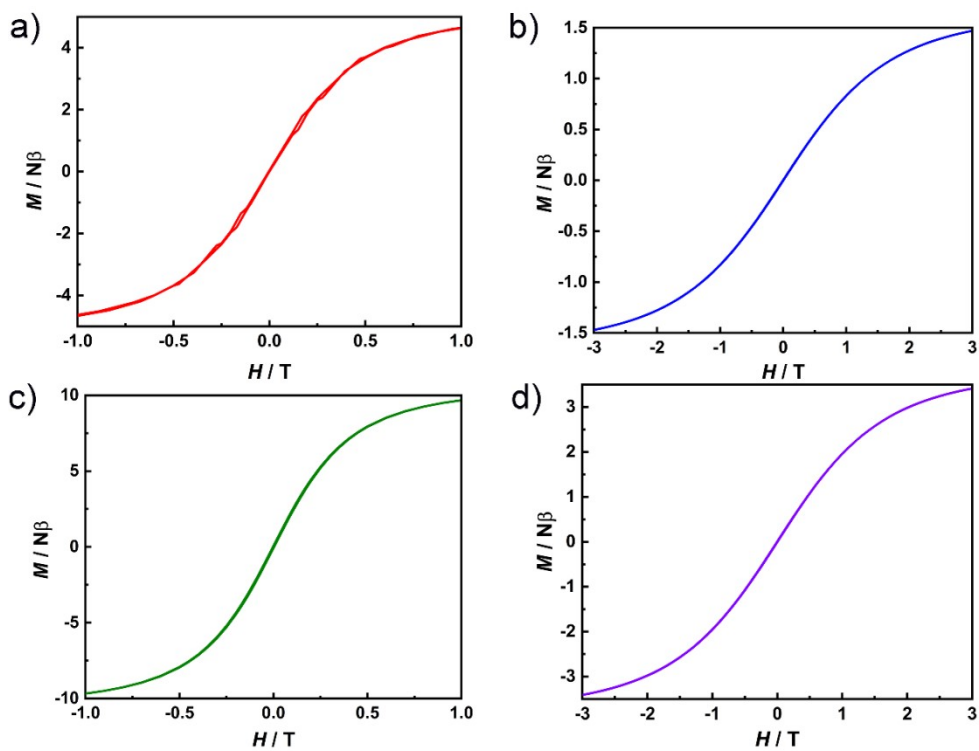


Fig. S13 Field dependence of the magnetization at 2 K for 1-4 (a-d).

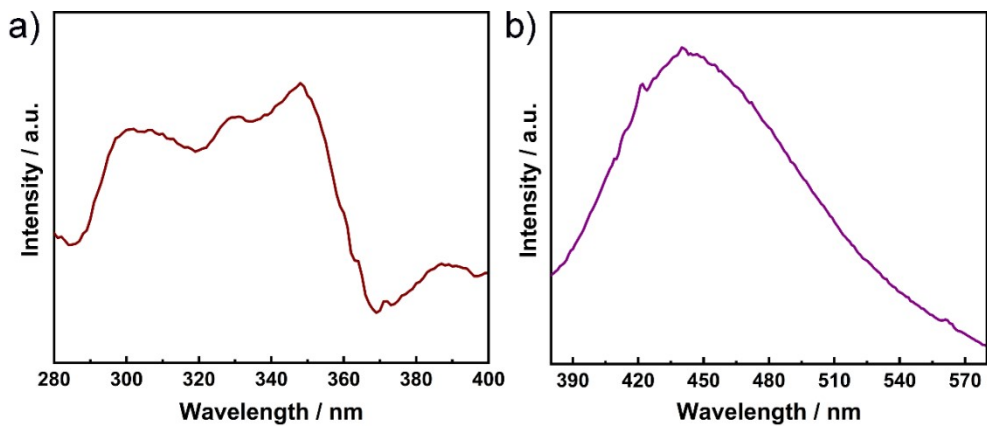


Fig. S14 Excitation (a) and emission spectra (b) of Hoqa ligand.

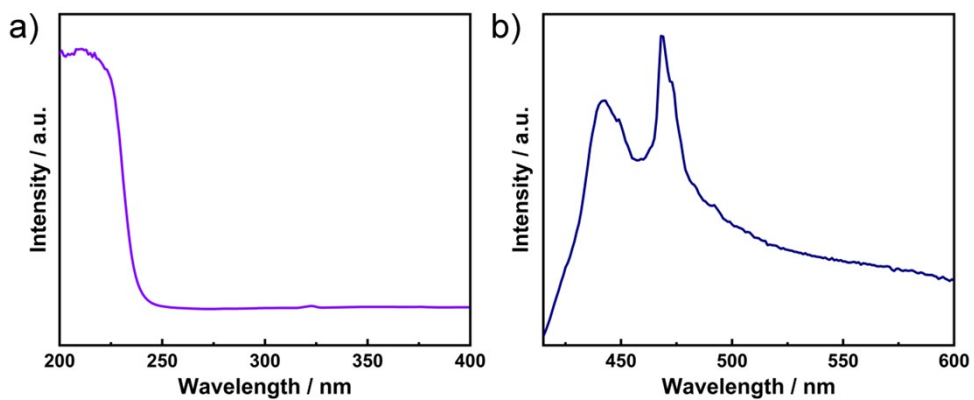


Fig. S15 Excitation (a) and emission spectra (b) of Hoaa ligand.

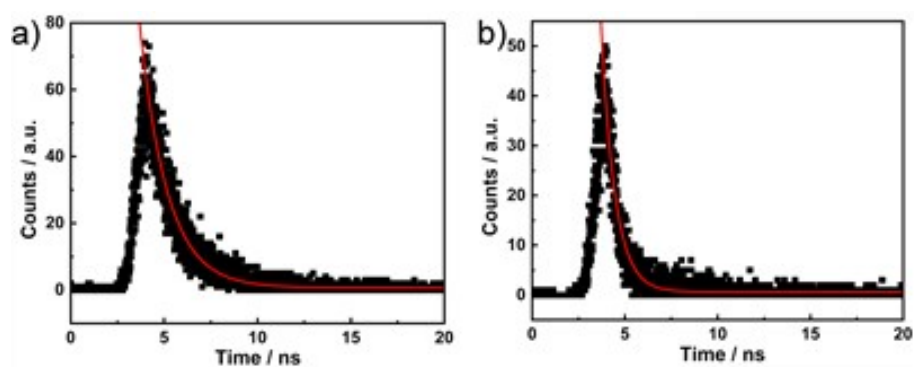


Fig. S16 Lifetime decay curves for Hoqa (a) and Hoaa (b) ligands. The red line is the best fit to a single exponential function.



(a)



(b)

Fig. S17 Images of **1** under day light (a) and UV light (b).

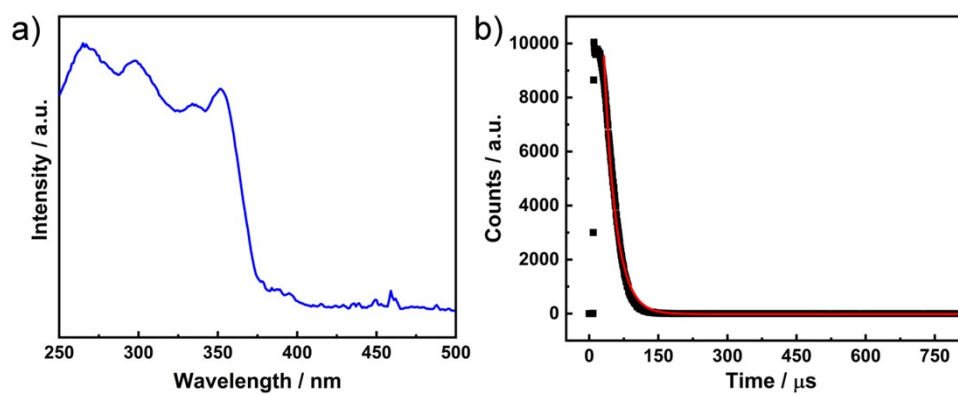


Fig. S18 Excitation spectrum (a) and Lifetime decay curve (b) of **1**. The red line is the best fit to a single exponential function.

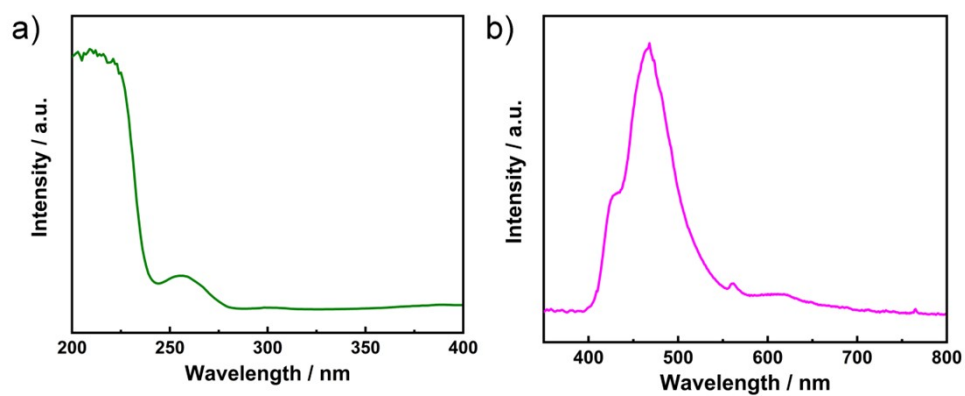


Fig. S19 Excitation (a) and emission spectra (b) of **3**.

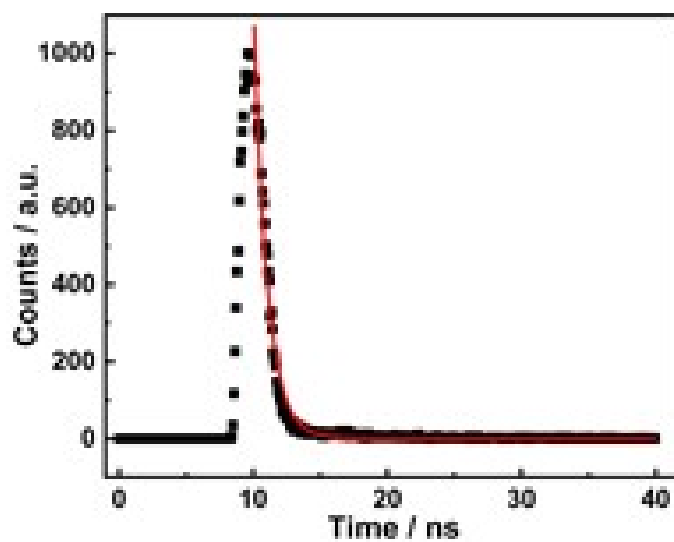


Fig. S20 Lifetime decay curve of **3**. The red line is the best fit to a single exponential function.

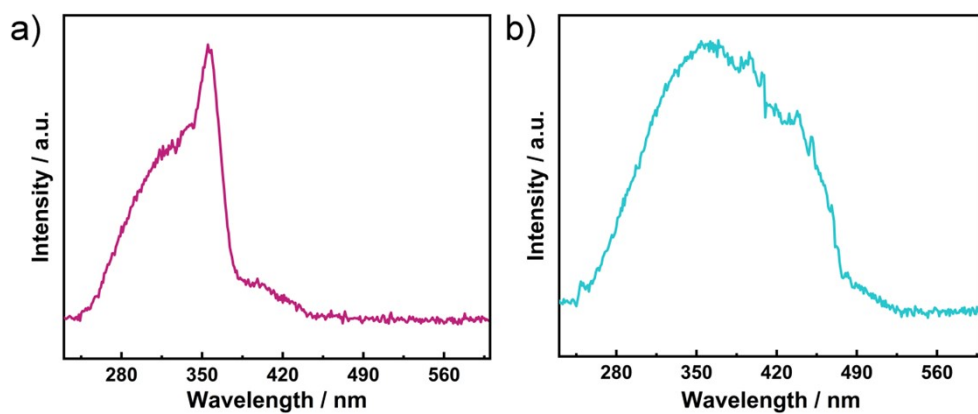


Fig. S21 Excitation spectra of **2** (a) and **4** (b).

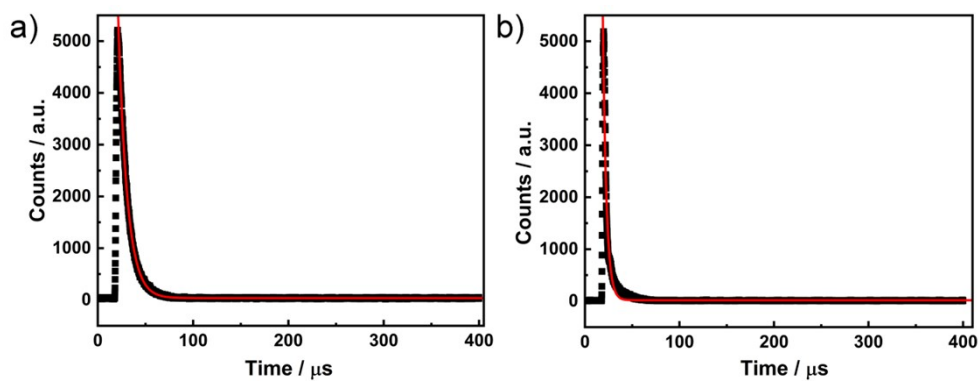


Fig. S22 Lifetime decay curves of **2** (a) and **4** (b). The red lines are the best fit to a single exponential function.